Eur. J. Mech., A/Solids, **14,** n° 3, 349-375, 1995

Ultimate bearing capacity of shallow foundations under inclined and eccentric loads. Part I: purely cohesive soil

J. SALENÇON* and A. PECKER**

ABSTRACT. – The problem of determining the bearing capacity of a strip footing resting on the surface of a homogeneous half space and subjected to an inclined, eccentric load is solved within the framework of the yield design theory, assuming the soil to be purely cohesive according to Tresca's strength criterion. The soil foundation interface is also purely cohesive, in terms of the homologous strength criterion.

Both the static and kinematic approaches of the yield design theory are used to derive lower and upper bounds for the ultimate bearing capacity. For an inclined centered load, an almost exact solution is derived; for increasing values of the load eccentricities, the ultimate bearing capacity can only be bracketed but nevertheless determined within a sufficient degree of accuracy from an engineering standpoint.

In a companion paper, the same problem is solved for a soil and an interface with a tension cut-off. These two solutions represent extreme conditions for the tensile resistance of the purely cohesive soil and could be used to bracket the variations of the bearing capacity as a function of the soil tensile strength.

1. Introduction

The problem solved in the current study, relates to the ultimate bearing capacity of a strip footing resting on the surface of a homogeneous half space and subjected to an inclined, eccentric load. The foundation, with width B, is assumed to have an infinite length and is subjected to uniformly distributed external loads along the direction Z (*Fig.* 1). It is also assumed to be rigid.

The ultimate bearing capacity (hereafter referred to as the bearing capacity) of the foundation is defined within the framework of the yield design theory, as detailed in [Salençon, 1983; 1993], using the yield strengths of the materials involved. It may be recalled that the practical relevance of such an analysis for a proper design depends on the possibility of simultaneously, where it is needed, mobilizing the resistance of the materials.

The soil underlying the foundation is purely cohesive with tensile strength. In the companion paper [Salençon, Pecker, 1995], the equivalent problem is solved for a cohesive soil with tension cut-off, *i.e.* without tensile strength.

The foundation interface is characterized by its strength criterion; the results presented in this paper are obtained for an interface without tensile strength and with a shear

* Professor, Laboratoire de Mécanique des Solides, École Polytechnique, 91128 Palaiseau Cedex, France.
** Chairman, Géodynamique et Structure, 157, rue des Blains, 92220 Bagneux, France.

EUROPEAN JOURNAL OF MECHANICS, A/SOLIDS, VOL. 14, N° 3, 1995
0997-7538/95/03/$ 4.00/© Gauthier-Villars

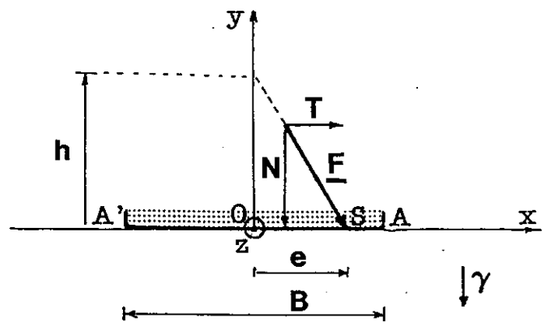

Fig. 1. – Strip foundation under inclined, eccentric load.

strength equal to the soil cohesion; however, results were similarly obtained, without any additional difficulty, for an interface with a limited tensile strength or with a shear strength different from that of the soil.

Using the assumptions listed above, the problem can be studied within the framework of the plane strain yield design theory, as defined in [Salençon, 1983].

Numerous publications (*i.e.* [Meyerhof, 1953; 1963, Hansen, 1961; 1970, Tran Vo Nhiem, 1971, Khosravi, 1983, Swami Saran and Argawal, 1991]) deal with the problem solved hereafter; however, load inclination and load eccentricity are seldom treated simultaneously. Moreover, in the proposed solution the foundation bearing capacity is computed with a very high degree of accuracy.

2. Problem modelization

2.1. Plane strain bearing capacity problem

The notations are given in Figure 1 where γ is the unit weight of the soil:

(1) $$\underline{\gamma} = -\gamma\, \underline{e}_y$$

and

(2) $$\underline{F} = -N\, \underline{e}_y + T\, \underline{e}_x, \qquad \underline{M} = -M\, \underline{e}_z$$

are the force system resultants, computed at 0, the mid-point of the foundation $A'A$; $\underline{e}_x, \underline{e}_y$ and $\underline{e}_z$ are the unit vectors of the cartesian coordinate axes Ox, Oy, Oz.

Let S be the point of application of $\underline{F}$ on Ox, and e, the algebraic eccentricity, which is positive along Ox; it follows that:

(3) $$M = Ne, \qquad |e| \leq B/2$$

In practical situations, the load eccentricity onto the foundation may arise due to an elevated point of application of the horizontal force component $\underline{T} = T\, \underline{e}_x$; hence:

(4) $$M = Th \qquad h \geq 0$$

The strength criterion for the homogeneous, purely cohesive halfspace ($y \leq 0$) is written as:

(5) $$f(\underline{\sigma}) = |\sigma_1 - \sigma_2| - 2C \leq 0$$

where σ_1 and σ_2 are the principal in-plane stresses of the stress tensor $\underline{\sigma}$; C designates the soil shear strength and tensile stresses are positive.

The strength criterion for the interface $A'A$, $y = 0$, $|x| < B/2$ is denoted as:

(6) $$f(\sigma_{xy}, \sigma_{yy}) = \mathrm{Sup}\,(|\sigma_{xy}| - C, \sigma_{yy}) \leq 0$$

The halfspace is subjected to the following boundary conditions:

- zero displacement at infinity

(7) $$y \leq 0, \quad |x| \to \infty : \quad \underline{U} = 0$$

- stress free boundary surface outside the foundation $A'A$

(8) $$y \leq 0, \quad |x| > B/2 : \quad \sigma_{yy} = \sigma_{xy} = 0$$

The external load, in addition to the gravity field, is applied on the upper face of the interface $A'A$ by the rigid foundation which implies that the velocity field $\underline{U}$ for $y = 0^+$, $|x| \leq B/2$ must correspond with a rigid body motion in the plane Oxy defined by its components in 0 : $\underline{U}_0$ and $\underline{\omega} = -\omega\, \underline{e}_z$.

It is straigthforward to check that the problem defined above depends on a finite number of loading parameters by expressing the principle of virtual work for any statically admissible stress field and any kinematically velocity field with the data $\underline{\gamma}$, $\underline{U}_0$ and $\underline{\omega}$:

(9) $$\mathfrak{p}_e(\underline{U}) = -\mathfrak{p}_i(\underline{U})$$

The virtual work for the external forces is given by:

(10) $$\mathfrak{p}_e(\underline{U}) = \underline{F}(\underline{\sigma}) \cdot \underline{U}_0 + \underline{M}(\underline{\sigma}) \cdot \underline{\omega} - \int_\Omega \gamma U_y \, \mathrm{d}\Omega$$

The loading parameters Q_i and associated kinematic parameters $\dot{q}_i$ are therefore:

$$(11)\qquad \begin{cases} Q_1(\underline{\underline{\sigma}}) = N(\underline{\underline{\sigma}}) = -\displaystyle\int_{A'A} \sigma_{yy}\, dx, & \dot{q}_1(\underline{U}) = -(U_0)_y \\ Q_2(\underline{\underline{\sigma}}) = T(\underline{\underline{\sigma}}) = \displaystyle\int_{A'A} \sigma_{xy}\, dx, & \dot{q}_2(\underline{U}) = (U_0)_x \\ Q_3(\underline{\underline{\sigma}}) = M(\underline{\underline{\sigma}}) = -\displaystyle\int_{A'A} x\,\sigma_{yy}\, dx, & \dot{q}_3(\underline{U}) = \omega \\ Q_4(\underline{\underline{\sigma}}) = \gamma, & \dot{q}_4(\underline{U}) = -\displaystyle\int_{\Omega} U_y(\underline{x})\, d\Omega \end{cases}$$

The virtual work of the internal forces is then:

$$(12)\qquad \mathfrak{p}_i(\underline{U}) = -\int_{\Omega} \underline{\underline{\sigma}} : \underline{\underline{d}}\, d\Omega - \int_{\Sigma} \underline{\underline{\sigma}} : (\llbracket \underline{U} \rrbracket \otimes \underline{n})\, d\Sigma - \int_{A'A} \underline{\underline{\sigma}} : (\llbracket \underline{U} \rrbracket \otimes \underline{e}_y)\, dx$$

where Ω represents the volume of the halfspace $y < 0$, Σ any line of discontinuity, if any, for the velocity field $\underline{U}$; and $\llbracket \underline{U} \rrbracket$, the velocity discontinuity when crossing Σ along the direction of its normal $\underline{n}$, or between the upper and lower faces of the interface $A'A$.

2.2. Fundamental results from the yield design theory

For the problem defined above, the yield design theory determines the set of all values for the four parameters N, T, M, γ, for which the equilibrium of the foundation is ensured without transgressing the strength criteria (5) and (6). Such values of (N, T, M, γ) are called potentially admissible or potentially safe parameters.

The foundation ultimate bearing capacity is defined by the boundary of the surface which, in the space (N, T, M), given γ and C, delineates the set of potentially safe loads.

The yield design theory gives methods for the determination or approximation of that boundary: a static approach "from inside", or a kinematic approach "from outside", which yield lower and upper bounds for the bearing capacity. The main statements are recalled hereafter for the particular case under study.

- **Static approach "from inside"**

The construction of a stress field $\underline{\underline{\sigma}}$, in equilibrium with the soil gravity forces and which complies with the strength criteria (5) in the soil and (6) at the interface, determines through (11), a loading $(N(\underline{\underline{\sigma}}), T(\underline{\underline{\sigma}}), M(\underline{\underline{\sigma}}))$ representing a lower bound for the foundation bearing capacity. The ultimate bearing capacity is, therefore, the envelope of all these determinations.

- **Kinematic approach "from outside"**

The concept of a maximum resisting work for the soil (resp. for the interface) is introduced from the virtual work $-\mathfrak{p}_i(\underline{U})$ in (12). The following functions are defined from the strength criteria of the materials:

- for the soil

$$(13)\qquad \begin{cases} \pi(\underline{\underline{d}}) = \mathrm{Sup}(\underline{\underline{\sigma}} :\ \underline{\underline{d}};\ f(\underline{\underline{\sigma}}) \le 0) \\ \pi(\underline{n}, \llbracket \underline{U} \rrbracket) = \mathrm{Sup}(\llbracket \underline{U} \rrbracket . \underline{\underline{\sigma}} . \underline{n};\ f(\underline{\underline{\sigma}}) \le 0) \\ \qquad\qquad = \pi(\llbracket \underline{U} \rrbracket \otimes \underline{n} + \underline{n} \otimes \llbracket \underline{U} \rrbracket)/2 \end{cases}$$

where $f(\underline{\underline{\sigma}})$ is given by (5).

- for the interface along $A'A$

$$(14)\qquad \{\pi(\llbracket \underline{U} \rrbracket) = \mathrm{Sup}(\sigma_{xy} \llbracket U_x \rrbracket + \sigma_{yy} \llbracket U_y \rrbracket;\ f(\sigma_{xy}, \sigma_{yy}) \le 0)$$

where $f(\sigma_{xy}, \sigma_{yy})$ is given by (6).

Any loading (N, T, M) whose work in some virtual, kinematically admissible, velocity field $\underline{U}$ is larger than the maximum resisting work minus the work of the gravity forces $\underline{\gamma}$ is an upper bound for the foundation ultimate bearing capacity. Hence, since $\underline{U}$ is kinematically admissible with the kinematic data $\underline{U}_0$ and ω, the inequality

$$(15)\qquad -N(U_0)_y + T(U_0)_x + M\omega \le \int_{\Omega} \pi(\underline{\underline{d}})\, d\Omega + \int_{\Sigma} \pi(\underline{n}, \llbracket \underline{U} \rrbracket)\, d\Sigma + \int_{A'A} \pi(\llbracket \underline{U} \rrbracket)\, dx + \int_{\Omega} \gamma U_y\, d\Omega$$

yields an upper bound for the foundation bearing capacity (N, T, M).

The plane strain expressions for $\pi(\underline{\underline{d}})$ and $\pi(\underline{n}, \llbracket \underline{U} \rrbracket)$ for the soil and $\pi(\llbracket \underline{U} \rrbracket)$ for the interface are recalled from [Salençon, 1983; 1993]:

- for a purely cohesive soil

$$(16)\qquad \begin{cases} \pi(\underline{\underline{d}}) = +\infty & \text{if } \mathrm{tr}\underline{\underline{d}} \ne 0 \\ \pi(\underline{\underline{d}}) = C(|d_1| + |d_2|) & \text{if } \mathrm{tr}\underline{\underline{d}} = 0 \end{cases}$$

$$(17)\qquad \begin{cases} \pi(\underline{n}, \llbracket \underline{U} \rrbracket) = +\infty & \text{if } \llbracket \underline{U} \rrbracket . \underline{n} \ne 0 \\ \pi(\underline{n}, \llbracket \underline{U} \rrbracket) = C|\llbracket \underline{U} \rrbracket| & \text{if } \llbracket \underline{U} \rrbracket . \underline{n} = 0 \end{cases}$$

- for the interface

$$(18)\qquad \begin{cases} \pi(\llbracket \underline{U} \rrbracket) = +\infty & \text{if } \llbracket U_y \rrbracket < 0 \\ \pi(\llbracket \underline{U} \rrbracket) = C \llbracket U_x \rrbracket & \text{if } \llbracket U_y \rrbracket \ge 0 \end{cases}$$

3. Fundamental results

3.1. Influence of the soil unit weight on the foundation bearing capacity

It can easily be shown that the bearing capacity of the foundation in the problem under consideration does not depend upon the soil unit weight. The proof follows the reasoning detailed in [Salençon, 1983] for the particular case of a vertical centered load specific to Tresca's yield criterion. From now on, the gravity forces will be set to zero, reducing the number of loading parameters to 3.

3.2. Convexity properties

– The convexity of the strength criteria (5) and (6) implies both the convexity of the domain of the potentially safe loads (N, T, M) and of its boundary which defines the bearing capacity;

– Results are conveniently presented in the plane (N, T) as the domain of the potentially safe loads for a given eccentricity e. The convexity of such domains stems from the preceding statement and from the definition of e in (3).

– Finally, for practical applications, the domain of stability is drawn in the (T, e) plane for a given N value. The convexity is ensured by the reasons stated above.

3.3. "$(1 - 2\,|\,e\,|/B)$ theorem" and method of the reduced width foundation

The following result follows from the static approach.

If the load $\underline{F}_0 = -N_0\,\underline{e}_y + T_0\,\underline{e}_x$ represents a value for the bearing capacity with zero eccentricity ($e = 0$), then the load $\underline{F} = \underline{F}_0(1 - 2\,|\,e\,|/B)$ represents a lower bound estimate for the bearing capacity with the load eccentricity e.

In fact, if $\underline{\underline{\sigma}}_0$ is a stress field in equilibrium with $\underline{F}_0$ which complies with the criteria (5) and (6), everywhere in the medium and along the interface, then $\underline{\underline{\sigma}}_e$ defined by:

$$(19)\qquad \underline{\underline{\sigma}}_e(x, y) = \underline{\underline{\sigma}}_0\left(\frac{x - e}{1 - 2\,|\,e\,|/B},\ \frac{y}{1 - 2\,|\,e\,|/B}\right),\quad \forall y \le 0,\quad \forall x,\quad |\,e\,| \le \frac{B}{2}$$

complies with the same criteria and is in equilibrium with the load $\underline{F}_0\,(1 - 2\,|\,e\,|/B)$ acting at an eccentricity e. As shown in Figure 2, this amounts to considering that the foundation with a reduced width $(B - 2\,|\,e\,|)$, with center S at the point of application of $\underline{F}$ on Ox, solely contributes to the bearing capacity of the foundation $A'A$, thus demonstrating a result which is usually admitted from heuristic considerations. This result is still valid even if $\underline{F}_0$ is a lower bound for the bearing capacity with $e = 0$.

3.4. Application

In the following, the bearing capacity for a foundation with a centric load will be estimated using both a static approach and a kinematic approach.

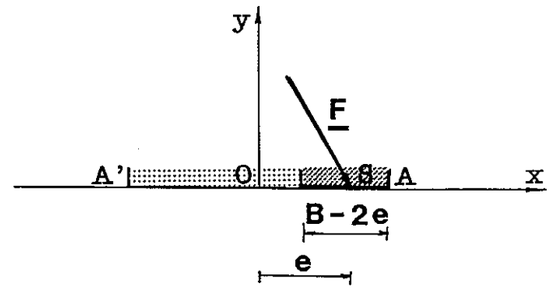

Fig. 2. – Reduced width foundation method.

The use of the results of paragraphs 3.2 and 3.3 (static approach) will then yield lower bound estimates for the eccentric load and new kinematic approaches will be derived to obtain upper bound solutions.

4. Bearing capacity for a centered load on a purely cohesive soil

4.1. Vertical load

The theoretical analysis is well known and only the main results are briefly recalled for use in the subsequent analyses.

The stress field given by [Prandtl, 1923] and extended by [Bishop, 1953], [Shield, 1954] and [Sayir-Ziegler, 1968] is in equilibrium with the weightless soil and complies with the strength criterion (5); along $A'A$ it is in equilibrium with the normal, compressive stress

$$(20)\qquad y = 0,\qquad |\,x\,| < B/2,\qquad \sigma_{yy} = -(\pi + 2)\,C,\qquad \sigma_{xy} = 0$$

thus complying with the strength criterion (6) for the interface (*Fig.* 6).

This stress field is associated with the classical, constant volume, velocity field $\underline{U}$ represented in Figure 3 where the soil boundary $A'A$ is subjected to a rigid body translation with velocity $\underline{V}$, inclined at the angle χ on Oy:

$$(21)\qquad \begin{cases} 0 \le |\,\chi\,| \le \pi/4, \\ \text{in } A'AB \quad \underline{U} = \underline{V} = V\,(\underline{e}_x\,\sin\,\chi - \underline{e}_y\,\cos\,\chi) \\ \text{in } ABC \quad U_\alpha = V\,\cos\,(\pi/4 - \chi), \quad U_\beta = 0 \\ \text{in } A'BC' \quad U_\alpha = 0, \quad U_\beta = -V\,\sin\,(\pi/4 - \chi) \\ \text{in } ACD \quad \underline{U} = V\,(\underline{e}_x + \underline{e}_y)\,\cos\,(\pi/4 - \chi)\,\sqrt{2}/2 \\ \text{in } A'C'D' \quad \underline{U} = V\,(-\underline{e}_x + \underline{e}_y)\,\sin\,(\pi/4 - \chi)\,\sqrt{2}/2 \end{cases}$$

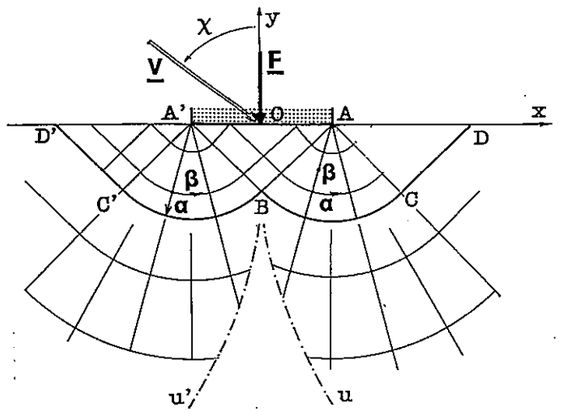

Fig. 3. – Prandtl's stress field: associated velocity fields ($|\chi| \leq \pi/4$); Shield's static extension.

where U_α and U_β represent the components of $\underline{U}$ in the orthonormal axes oriented along the lines α and β at the current point. The velocity is continuous across the interface $A'A$ and the soil medium is motionless below $D'C'BCD$.

The inequality (15) then becomes:

$$\begin{cases} \underline{F}.\underline{V} = V(N \cos\chi + T \sin\chi) \leq VCB(\pi+2)\cos\chi \\ V > 0, \qquad |\chi| \leq \pi/4 \end{cases} \tag{22}$$

which yields an upper bound for the bearing capacity. When compared with the static approach, it yields the exact value for the bearing capacity for a foundation under a vertical centric load:

$$N = (\pi+2)\,CB, \qquad T = 0, \qquad M = 0. \tag{23}$$

4.2. Inclined load: kinematic approaches

- **Bilateral velocity fields**

The velocity fields defined by equations (21) bound the bearing capacity for an inclined load through equation (22). The best upper bound is obtained when $|\chi| = \pi/4$:

$$(N + |T|) \leq (\pi+2)\,CB. \tag{24}$$

- **Unilateral velocity fields**

The velocity field sketched in Figure 4 is now considered, where the foundation and the volume $A'AB$ are given a rigid body translation motion with the velocity $\underline{V}$ parallel

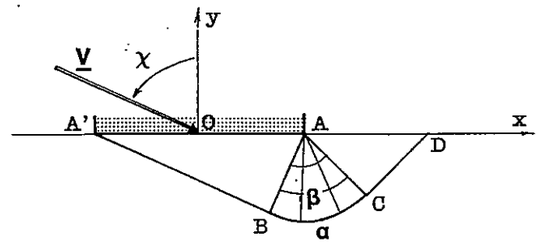

Fig. 4. – Unilateral velocity fields ($\pi/4 \leq |\chi| \leq \pi/2$).

to $A'B$ (or, symmetrically, AB according to the sign of χ); the soil medium below $A'BCD$ is motionless; the volume ACD moves parallel to CD with the velocity V; a velocity jump with a magnitude of V occurs along $A'BCD$ and the velocity field in ABC is written as:

$$\begin{cases} \pi/4 \leq |\chi| \leq \pi/2 \\ \underline{V} = V(\underline{e}_x \sin\chi - \underline{e}_y \cos\chi) \\ U_\alpha = V, \quad U_\beta = 0 \end{cases} \tag{25}$$

The inequality (15) is then:

$$\begin{cases} \underline{F}.\underline{V} = V(N\cos\chi + T\sin\chi) \leq VCB(\sin|\chi| \\ \quad + (3\pi/2 + 1 - 2|\chi|)\cos\chi) \\ \pi/4 \leq |\chi| \leq \pi/2 \end{cases} \tag{26}$$

The bearing capacity is therefore bounded by a family of two straight lines in the (N, T) plane which envelop cycloidal arcs with equations

$$\begin{cases} N/CB = 3\pi/2 + 1 - 2|\chi| + \sin 2|\chi| \\ T/CB = -(\chi/|\chi|)\cos 2\chi \\ \pi/4 \leq |\chi| \leq \pi/2 \end{cases} \tag{27}$$

and extend with the segments:

$$\begin{cases} 0 \leq N/CB \leq 1 + \pi/2 \\ |T|/CB = 1 \end{cases} \tag{28}$$

For $|\chi| = \pi/4$, this result agrees with that obtained in the kinematic approach (*Fig.* 8). For $|\chi| = \pi/2$, the velocity field breaks down into a solution where there is a sliding of the foundation, parallel to the interface $A'A$ and the velocity jump takes place within the soil immediately below the interface, while the remainder of the soil mass stays motionless.

4.3. INCLINED LOAD: STATIC APPROACH FROM INSIDE

• Purely tangential load

The discontinuous stress field proposed by Khosravi and Salençon [Khosravi, 1983] is presented in Figure 5. Within the axes (OX, OY) rotated by $\pi/4$ from (Ox, Oy) this field is given by:

$$(29)\qquad \begin{cases} \text{zone 1} & \sigma_{XX} = C, \quad \sigma_{YY} = -C, \quad \sigma_{XY} = 0 \\ \text{zone 2} & \sigma_{XX} = 0, \quad \sigma_{YY} = -C, \quad \sigma_{XY} = 0 \\ \text{zone 3} & \sigma_{XX} = C, \quad \sigma_{YY} = 0, \quad \sigma_{XY} = 0 \\ \text{zones 4, 5, 6} & \sigma_{XX} = 0, \quad \sigma_{YY} = 0, \quad \sigma_{XY} = 0 \end{cases}$$

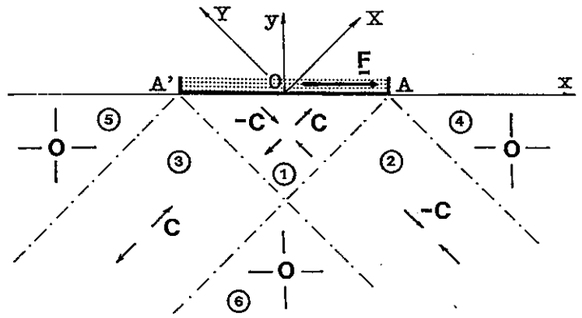

Fig. 5. – Stress field with six zones in equilibrium with a purely tangential load.

The field is in equilibrium with the weightless soil and complies with the strength criteria (5) anywhere in the soil and (6) along the interface. Along $A'A$:

$$(30)\qquad \sigma_{YY} = 0, \qquad \sigma_{XY} = C$$

It is in equilibrium with the loads

$$(31)\qquad N(\underline{\sigma}) = 0, \qquad T(\underline{\sigma}) = CB, \qquad M(\underline{\sigma}) = 0$$

• Arbitrary inclined load

A static solution has been constructed by Khosravi and Salençon [Khosravi, 1983]. It is based on the classical results for the bearing capacity of an infinite trapezoidal purely cohesive, weightless wedge $t'B'Bt$, with a vertex angle 2α, subjected along $B'B$, to a uniform normal stress Σ (positive in tension); the faces $t'B'$ and tB are stress free.

Figure 6 recalls that the association of the Prandtl velocity field with the corresponding stress field, extended by Bishop's or Shield's methods, results in the exact value of this bearing capacity:

$$(32)\qquad |\Sigma| = 2C(1+\alpha)$$

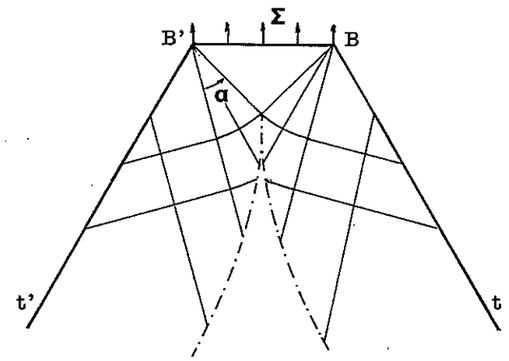

Fig. 6. – Trapezoidal wedge with apex angle 2α. Bearing capacity from Prandtl's stress fields and Shield's criterion.

Let $\underline{\underline{\sigma}}_s(\alpha)$ be the stress field, sketched in Figure 6, obtained by Shield's method, which is in equilibrium with the uniform stress $\Sigma = 2C(1+\alpha)$ equal to the bearing capacity in tension. The stress field for the static approach of the bearing capacity under an inclined load is defined as follows (*Fig.* 7):

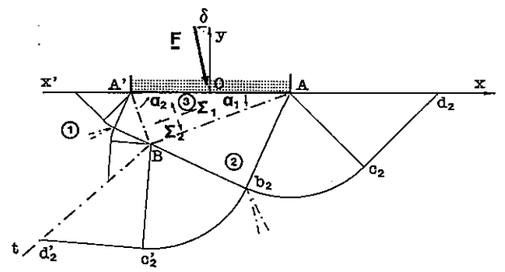

Fig. 7. – Bearing capacity under inclined load: static approach.

– zone 3 is a right-angled triangle $A'BA$ where $\underline{\underline{\sigma}}_3$ is a homogenous field whose principal stresses are Σ_1 parallel to AB and Σ_2 parallel to $A'B$;

– zone 1 is a symmetrical infinite trapezoidal wedge $x'A'Bt$, with a vertex angle $2\alpha_1$, where the stress field is $\underline{\underline{\sigma}}_1$

$$\underline{\underline{\sigma}}_1 = \frac{\Sigma_1}{2C(1+\alpha_1)}\,\underline{\underline{\sigma}}_s(\alpha_1) = \frac{C_1}{C}\,\underline{\underline{\sigma}}_s(\alpha_1) \tag{33}$$

in which

$$\Sigma_1 = 2C_1(1+\alpha_1) \tag{34}$$

– zone 2 is another symmetrical infinite trapezoidal wedge $tBAx$, with an apex angle $2\alpha_2 = \pi - 2\alpha_1$, where the stress field is:

$$\underline{\underline{\sigma}}_2 = \frac{\Sigma_2}{2C(1+\alpha_2)}\,\underline{\underline{\sigma}}_s(\alpha_2) = \frac{C_2}{C}\,\underline{\underline{\sigma}}_s(\alpha_2) \tag{35}$$

in which

$$\Sigma_2 = 2C_2(1+\alpha_2). \tag{36}$$

This field is obviously in equilibrium throughout the weightless soil medium. Along $A'A$, the stresses:

$$\begin{aligned}\sigma_{yy} &= (\Sigma_2+\Sigma_1)/2 + ((\Sigma_2-\Sigma_1)\cos 2\alpha_1)/2\\ \sigma_{xy} &= ((\Sigma_1-\Sigma_2)\sin 2\alpha_1)/2\end{aligned} \tag{37}$$

develop.

The strength criterion (5) imposes the following constraints:

$$|\Sigma_2-\Sigma_1|/2 = \left|C_2\left(1+\frac{\pi}{2}-\alpha_1\right) - C_1(1+\alpha_1)\right| \le C, \tag{38}$$

$$|C_1| \le C, \tag{39}$$

$$|C_2| \le C. \tag{40}$$

In view of (38), the strength criterion for the interface will be satisfied if:

$$(\Sigma_2+\Sigma_1)/2 + ((\Sigma_2-\Sigma_1)\cos 2\alpha_1)/2 \le 0 \tag{41}$$

also holds.

The family of stress fields under consideration depends upon three parameters α_1, C_1/C, C_2/C, with the constraints (38) to (41). It yields the following lower bounds for the bearing capacity:

$$\begin{cases} N(\underline{\underline{\sigma}}) = -B(\Sigma_1+\Sigma_2-(\Sigma_1-\Sigma_2)\cos 2\alpha_1)/2\\ T(\underline{\underline{\sigma}}) = B(\Sigma_1-\Sigma_2)\sin 2\alpha_1/2\\ M(\underline{\underline{\sigma}}) = 0 \end{cases} \tag{42}$$

Retaining the convex envelope and taking into account the exact value of the bearing capacity already obtained for the case of an axial load, the lower bound for the bearing capacity for any centric loading consists of three arcs and their symmetrical solutions shown in Figure 8, whose equations are:

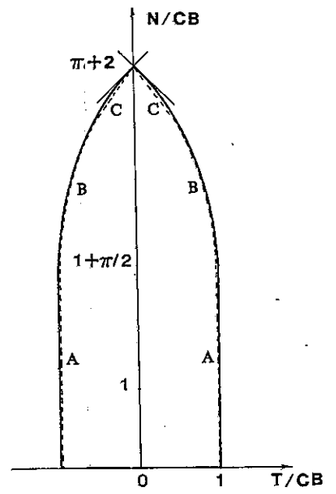

Fig. 8. – Bearing capacity under centered inclined load.
Solid lines: upper bound estimate. Dotted lines: lower bound estimate.

Arc A:

$$\begin{cases} N/CB = 1-(\pi+4)C_1/2C\\ T/CB = 1\\ -\pi/(\pi+4) \le C_1/C \le 2/(\pi+4)\\ (\alpha_1 = \pi/4,\ C_2/C = C_1/C - 4/(\pi+4)) \end{cases} \tag{43}$$

Arc B:

$$(44)\qquad \begin{cases} N/CB = \pi + 1 - 2\,\alpha_1 + \cos 2\,\alpha_1 \\ T/CB = \sin 2\,\alpha_1 \\ \pi/4 - 1/2 \le \alpha_1 \le \pi/4 \\ (C_1/C = (\alpha_1 - \pi/2)/(\alpha_1 + 1),\ C_2/C = -1) \end{cases}$$

Arc C:

$$(45)\qquad \begin{cases} N/CB = (\pi + 2) - \lambda\,(\pi/2 - \sin 1) \\ T/CB = \lambda \cos 1 \\ 0 \le \lambda \le 1 \end{cases}$$

It is worth noting that along the arc A, the strength criterion of the soil is reached, *i.e.* equality in equation (5), in zone 3 only; in particular, for $\alpha_1 = \pi/4$, and $C_1/C = 2/(\pi + 4)$, a stress field, different to that of Figure 5, is obtained, which is in equilibrium with a purely tangential load. Along the arc B, the strength criterion of the soil is reached in zones 2 and 3; in the former, the field $\underline{\underline{\sigma}}_2 = -\underline{\underline{\sigma}}_s\,(\alpha_2)$ is homogeneous throughout ABb_2 and identical to $\underline{\underline{\sigma}}_3$ from zone 3. For $\alpha_1 = \pi/4 - 1/2$, the strength criterion of the soil is reached simultaneously in all three zones ($C_1 = C_2 = -C$).

4.4. Bearing capacity for an inclined load

The comparison of the results of both approaches, given in Figure 8 shows that both approaches yield the same result along the arcs A, B and at point ν_0. An algebraic check is straigthforward if one notes that for the arc B, for instance, equations (27) for $\pi/2 - 1/2 \le \chi \le \pi/2$ and (44) for $\pi/4 - 1/2 \le \alpha_1 \le \pi/4$ define the same cycloidal arc, α_1 and χ being related by:

$$(46)\qquad \chi - \alpha_1 = \pi/4$$

As expected from the association theorem of the theory of yield design, it turns out that the optimal stress field corresponding to the arc B given by (44) and the unilateral velocity field, are associated when α_1 and χ are related through (46).

Denoting δ as the load inclination defined by:

$$(47)\qquad \tan\delta = T/N,$$

the preceding analysis yields

– the exact value of the bearing capacity for $\delta = 0$ (axial load) and for $7° \le \delta \le 90°$,

– an estimate within an error of 0.6% for a fixed δ, for $0 < \delta < 7°$.

It may be anticipated that the result from the kinematic approach yields the exact value and that an exact solution for $0 < \delta < 7°$ could be obtained through a more refined static analysis. Such a solution would be purely academic and not particularly useful for practical applications. The accuracy of the stress fields of Figure 7 is remarkable.

In fact, a comparison made by [Khosravi, 1983] shows that the values proposed by [Meyerhof, 1953], [Tran Vo Nhiem, 1968, 1971], [Mirzabekian, 1979] coincide exactly with the results (equations (27) and (28)) of Figure 8 if N is expressed as a function of δ. Paragraph 4.2 of the present study states that these values are upper bounds and it follows that Meyerhof's formula [Meyerhof, 1963], which reduces the normal bearing capacity by the factor $(1 - \delta/2\pi)^2$, becomes questionable as soon as $8° \le \delta \le 60°$ since it may overestimate the bearing capacity by a factor of up to 30% for specific values of δ (*Fig.* 9). Paragraph 4.3, as a result of the accuracy of the static approaches, fully justifies, from a theoretical viewpoint, the use of the values given by equations (27) and (28), recommended for instance by [Giroud, Tran Vo Nhiem and Obin, 1973]. It shows that the formulae proposed by [Brinch Hansen, 1961, 1970] slightly underestimate the bearing capacity for low angles of load inclination; as does Meyerhof's formula. It also points out that the Meyerhof formula underestimates the bearing capacity for high angles of load inclination, since Meyerhof predicts a nil bearing capacity for a purely tangential load. Our results show definitively that the bearing capacity is $|T| = CB$ for $N = 0$.

However, the reader's attention must be drawn to the fact that the latter result for the tangential bearing capacity essentially depends upon the strength criterion (6) adopted for the interface $A'A$; as shown in [Khosravi, 1983], the consideration of a Coulomb criterion for the interface leads to a truncation of the domain in the (N, T) plane with

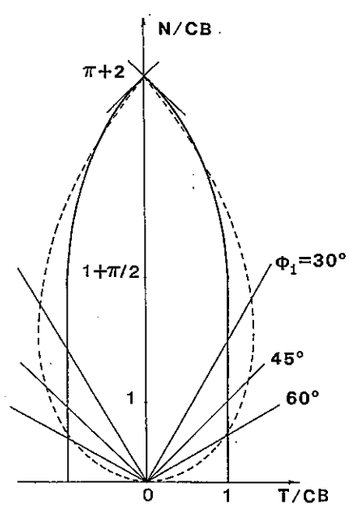

Fig. 9. – Inclined centered load: comparison with Meyerhof's formula (1953).

straight lines $|T| = N \tan \phi_i$ where ϕ_i represents the friction angle of the interface (*Fig.* 9). This question will be considered again in Section 5.

Finally, it is worth noting that the format of the formulae proposed in the literature gives the normal load as a function of the load inclination; even if the computation of the tangential load is straightforward using equation (47), it is interesting to draw the diagram in the (N, T) plane, since it highlights the sensitivity of both components to the load inclination.

5. Bearing capacity for an inclined, eccentric load

5.1. Static approach from inside

• Application of the reduced width foundation method

Starting from the diagram in Figure 8, the reduced width foundation method yields a lower bound estimate for any value of the eccentricity e ($|e| < B/2$) by applying the similarity of center 0 and of ratio $(1 - 2|e|/B)$ to the arcs A, B, C (and to the symmetrical ones) in the (N, T) plane, as shown in Figure 10.

• Use of convexity

The convexity, in the (N, T, M) plane, of the domain of (potentially) safe loads makes it possible to improve the above results. In fact, since $M = Ne$ (equation 3),

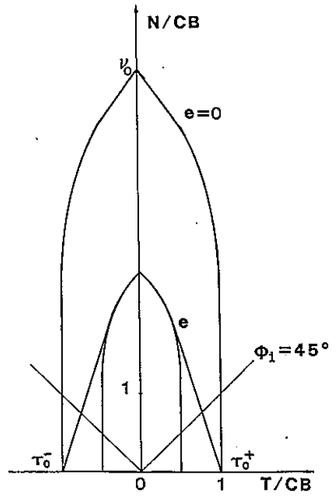

Fig. 10. – Inclined eccentric load: static approach from the reduced width foundation method and convexity properties.

it can be stated that: with any (N_1, T_1) and any (N_2, T_2) corresponding to lower bound estimates of the bearing capacity for eccentricities e_1 and e_2 respectively, and any λ, $0 \leq \lambda \leq 1$, then, the load

$$N = \lambda N_1 + (1 - \lambda) N_2, \qquad T = \lambda T_1 + (1 - \lambda) T_2 \tag{48}$$

represents a lower bound estimate of the bearing capacity for the eccentricity:

$$e = \frac{\lambda N_1 e_1 + (1 - \lambda) N_2 e_2}{\lambda N_1 + (1 - \lambda) N_2} \tag{49}$$

A direct application of this result considers, on one hand, the lower bound approach obtained by the reduced width foundation method for the eccentricity $e_1 = e$, and on the other hand, the loads $(N = 0, |T| = CB)$ represented by the points τ_0^+ and τ_0^- associated with the bearing capacity under a purely tangential load for $e_2 = 0$. From (48) and (49), we find that the convex envelope of the lower bound approach obtained by the reduced width foundation method on one hand and with points τ_0^+ and τ_0^- on the other hand, is itself a lower bound estimate of the bearing capacity for the same eccentricity e: if (N, T) is (potentially) safe for e, so is $(\lambda N, \lambda T \mp (1 - \lambda) CB)$.

A systematic numerical exploration of formulae (48) and (49) did not improve the aforementioned results which are sketched in Figure 10.

This result is of paramount importance since it demonstrates that the reduced width foundation method associated with the reduction factor $(1-2|e|/B)$, which is commonly recommended in practice [Giroud, Tran Vo Nhiem, Obin, 1973], may significantly underestimate the bearing capacity for large eccentricities.

However, it should be observed, that like points τ_0^+ and τ_0^-, the validity of this result is closely related to the strength criterion (6) assumed for the interface. It can easily be checked that for a different interface strength criterion (for instance a Coulomb interface), the diagrams of Figure 10 should be truncated, as in Figure 9, by the representation of the criterion expressed in terms of N/CB and T/CB instead of σ_{yy} and σ_{xy}.

5.2. Kinematic approaches

• A straightforward upper bound

The bilateral velocity fields of Figure 3 and the unilateral ones of Figure 4 are associated with a rigid body translation, with velocity $\underline{V}$, of the upper face of the interface $A'A$. It follows that the loading parameter M does not appear in the work done by the external forces in the inequalities (22) and (26); in other words, this work does not depend upon the eccentricity e. Consequently, the upper bound obtained in paragraph 4 and represented in Figure 8 remains valid for an eccentric load.

To improve this result, Pecker and Salençon (1991a) proposed different original velocity fields which yield better upper bounds for the foundation bearing capacity, depending on the values of the inclination of the load or of the eccentricity.

A brief, concise description of these fields is given hereafter. The description will be used in the computation of the maximum resisting work which is found on the right hand side of inequality (15); the derivation of these expressions is still based on formulae (16) and (17) for the soil and (18) for the interface, which are expressions of the functions $\pi(.)$ given in equation (15). The results derived for the foundation bearing capacity are presented for different eccentricities in the form of diagrams in the (N, T) plane. Only positive values for the eccentricity are considered ($0 \leq e \leq B/2$); the results for a negative eccentricity are obtained by changing e into $-e$, δ into $-\delta$ and T into $-T$.

- **Mechanism A**

Mechanism A is presented in Figure 11. The velocity field $\underline{U}$ is the description of:

– a rigid body rotation, with angular velocity $\underline{\omega} = -\omega\, \underline{e}_z$ ($\omega > 0$), around the point Ω, for the lower face of the interface $A'A$ along the segment IA and for the volume IJA delimited by the arc IJ of a circle centered at Ω and tangential to $A'A$ at I; point I is assumed to lay between A' and A;

– a shear zone AJK delimited by the arc of circle JK centered at A;

– a shear zone AKL;

– a constant tangential velocity discontinuity $\underline{V}$ across the line $IJKL$, with the soil medium below that line being motionless.

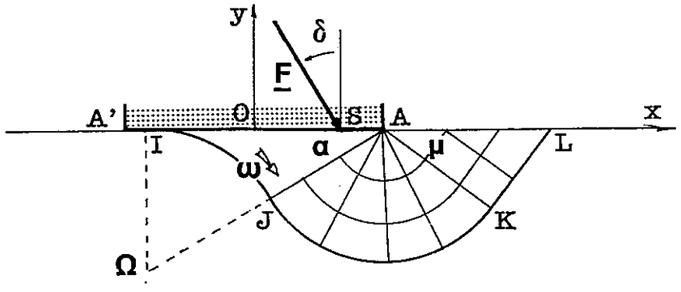

Fig. 11. – Mechanism A.

The upper face of the foundation interface $A'A$, *i.e.* the foundation itself, moves in the same rigid body rotation around Ω with an angular velocity $\underline{\omega}$; separation between both faces of the interface $A'A$ takes place within the interface along the segment $A'I$; the velocity is then continuous across IA.

This velocity field depends upon three parameters: the angles α and μ (*Fig.* 11) which define the directions $A\Omega$ and AK and the scalar λ which positions I on $A'A$:

$$\underline{IA} = \lambda B \underline{e}_x \tag{50}$$

The inequality (15) is written as:

$$\begin{cases} \underline{F}.\underline{U}_0 + \underline{M}.\underline{\omega} = \omega\,[(\lambda + e/B - 1/2)\,N + \lambda T\,\tan\,\alpha] \\ \leq \omega\, CB\,\lambda\,(1-\lambda)\,\tan\,\alpha \\ +\omega\, CB\,\lambda^2\,(\pi/2 - \mu + (\tan\,\mu)/2 + (\pi/2 - \alpha)/\cos^2\,\alpha) \end{cases} \tag{51}$$

The minimization is first carried out on the right hand side of the equation with respect to μ, which gives $\mu = \pi/4$. Then, one can proceed, for a fixed δ, to minimize the right hand side of:

$$\frac{N}{CB} \leq \frac{\lambda^2\,[\pi/4 + 1/2 + (\pi/2 - \alpha)/\cos^2\,\alpha] + \lambda\,(1-\lambda)\,\tan\,\alpha}{\lambda\,(1 + \tan\,\delta\,\tan\,\alpha) + e/B - 1/2} \tag{52}$$

under the constraints on α and λ

$$(1/2 - e/B)/(1 + \tan\,\delta\,\tan\,\alpha) < \lambda \leq 1 \tag{53}$$

- **Mechanism B**

Mechanism B is shown in Figure 12; it is similar to the mechanism A but point I, defined by (50), is now located left of point A', *i.e.* $\lambda > 1$. The velocity field does no longer present a velocity discontinuity across the interface $A'A$. It depends upon three parameters: the angles α, β and μ, which define the directions $A\Omega$, $A'\Omega$ and AK.

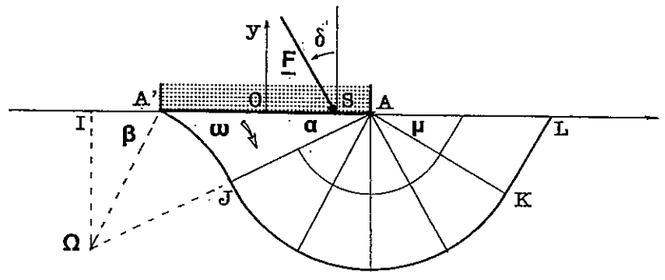

Fig. 12. – Mechanism B.

The inequality (15) becomes:

$$\begin{aligned} &\left(\frac{\tan\,\beta}{\tan\,\beta - \tan\,\alpha} + \frac{e}{B} - \frac{1}{2}\right)\frac{N}{CB} + \frac{\tan\,\alpha\,\tan\,\beta}{\tan\,\beta - \tan\,\alpha}\,\frac{T}{CB} \\ &\leq \frac{\tan^2\,\beta}{(\tan\,\beta - \tan\,\alpha)^2}\left[\left(\pi - \mu + \frac{1}{2}\,\tan\,\mu\right)\left(1 - \frac{\sin^2\,\alpha}{\sin^2\,\beta}\right)\right. \\ &\left.\left[+\beta\,\frac{\sin^2\,\alpha}{\sin^2\,\beta} - \alpha\right]\frac{1}{\cos^2\,\alpha}\right. \end{aligned} \tag{54}$$

The minimization with respect to μ is trivial: $\mu = \pi/4$. For a fixed δ, minimization is carried on the right hand side of:

$$(55)\quad \frac{N}{CB} \leq \frac{[\tan^2\beta\,(3\pi/4+1/2)\,(1-\sin^2\alpha/\sin^2\beta)+\beta\,\sin^2\alpha/\sin^2\beta-\alpha]}{\cos^2\alpha\,(\tan\beta-\tan\alpha)\,[\tan\beta\,(1+\tan\delta\,\tan\alpha)+(e/B-1/2)\,(\tan\beta-\tan\alpha)]}$$

under the geometrical constraints on α and β

$$(56)\quad \begin{gathered} 0<\alpha<\beta<\pi/2 \\ \tan\beta\,(1+\tan\delta\,\tan\alpha)+(e/B-1/2)\,(\tan\beta-\tan\alpha)>0 \end{gathered}$$

The conditions (56) state that mechanism B is defined only if $\alpha < \beta$. However, if $\alpha = \beta$, this mechanism breaks down to the unilateral mechanism of Figure 8 with $\chi = \alpha$. This is confirmed by the limit value of equation (55) when β tends to α

$$(57)\quad N/CB \leq (3\pi/2+1+\tan\alpha-2\,\alpha)/(1+\tan\alpha\,\tan\delta)$$

which does not depend upon e and whose right hand side should be minimized with respect to α, δ being fixed. Then for $\delta > 0$:

$$\tan\delta = -\cos 2\alpha/(3\pi/2+1-2\,\alpha+\sin 2\alpha), \qquad \pi/4<\alpha<\pi/2$$

which yields

$$N/CB \leq 3\pi/2+1-2\,\alpha+\sin 2\alpha$$
$$T/CB \leq -\cos 2\alpha$$

For $\delta < 0$, the same formulae are still valid with $0 < \alpha < \pi/4$.

- **Mechanism C**

Mechanism C is presented in Figure 13. This velocity field describes a rigid body rotational motion with angular velocity $\underline{\omega} = -\omega\,\underline{e}_z$ $(\omega > 0)$ around point Ω for the lower face of the interface $A'A$ along the segment aA and for the volume $AIaA$ delimited by the arc Aa of a circle centered at Ω. Point I on Ox, the vertical projection of Ω, is located between 0 and A; it is defined by equation (50) with $0 < \lambda < 1/2$. The velocity $\underline{U}$ is discontinuous across the arc of circle Aa, the soil medium below Aa being motionless.

The upper face of the interface $A'A$, *i.e.* the foundation, moves in the same rigid body rotation around Ω with velocity $\underline{\omega}$; separation between both faces of the interface $A'A$ takes place along $A'a$ within the interface; the velocity is continuous along aA.

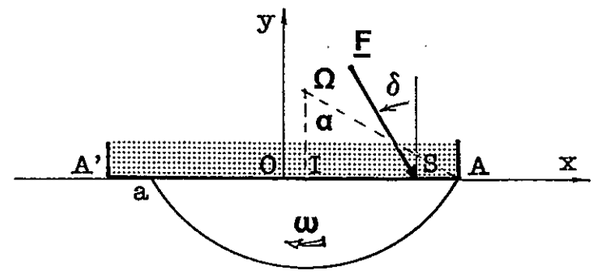

Fig. 13. – Mechanism C.

This velocity field depends upon two parameters: the scalar λ and the angle α which defines the direction $A\Omega$. The inequality (15) leads to the minimization with respect to λ and α, δ being fixed, of the right hand side of:

$$(58)\quad \frac{N}{CB} \leq 2\,\lambda\,\frac{\lambda\alpha/\sin^2\alpha+(1/2-\lambda)/\tan\alpha}{\lambda\,(1-\tan\delta/\tan\alpha)+e/B-1/2}$$

under the constraints

$$(59)\quad \begin{cases} 0<\alpha<\pi/2 \\ 0<\lambda<1/2, \qquad (1/2-e/B)/(1-\tan\delta/\tan\alpha)<\lambda \end{cases}$$

- **Mechanism D**

Mechanism D is presented in Figure 14. It is similar to the previous mechanism but $\lambda > 1/2$: hence point a is no longer between A' and A and the velocity is continuous across $A'A$.

The inequality (58) becomes:

$$(60)\quad \frac{N}{CB} \leq \frac{2\,\lambda^2\,\alpha/\sin^2\alpha}{\lambda\,(1-\tan\delta/\tan\alpha)+e/B-1/2}$$

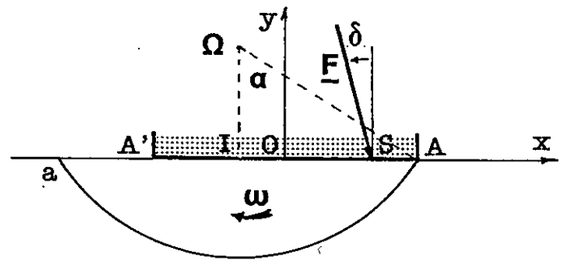

Fig. 14. – Mechanism D.

and is minimized, for a fixed δ, under the constraints:

$$(61) \qquad \begin{cases} 0 < \alpha < \pi/2 \\ 1/2 < \lambda, \qquad (1/2 - e/B)/(1 - \tan\delta/\tan\alpha) < \lambda \end{cases}$$

- **Additional mechanisms**

The constraint $e/B > 0$, adopted for the presentation of the results, is not significant in the study of the mechanisms themselves. All the derived formulae, such as (52) and (53), (55) and (56), (58) and (59), (60) and (61), are valid for the whole range $-1/2 \leq e/B \leq 1/2$.

Advantage can be taken of this remark. For $0 < e/B < 1/2$, without any additional algebraic computations, the mechanisms A', B', C', D', which are symmetrical about the axis Oy to the mechanisms A, B, C, D, can be studied by changing e into $(-e)$, T into $(-T)$ and δ into $(-\delta)$.

In addition to these four additional mechanisms, another mechanism E , which is presented in Figure 15, has also been studied. It is closely related to mechanism A, with slipping developing within the interface $A'A$ along IA: the velocity is continuous across $IJKL$ and shear takes place within the volume delimited by the line $IJKL$. Analytical and numerical calculations were performed on mechanism E which depends upon three parameters, and on mechanism F which is similar to E but is relevant to the case where I lies outside $A'A$. The results turn out to be less accurate than those of mechanisms A and B: N/CB values are slightly higher for a fixed δ. The algebraic expressions for these mechanisms can be found in [Pecker-Salençon, 1991a].

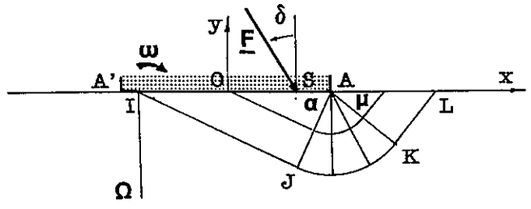

Fig. 15. – Mechanism E.

- **Summary of results**

The overall picture of the results obtained by the kinematic approach for all the preceding mechanisms is presented in Figure 16. Curves for the best upper bounds for the bearing capacity are given for load eccentricities e/B =0, 0.1, 0.2, 0.3, 0.4. Each curve is composed of different arcs which are detailled hereafter.

All the vertical lines with the abscissa $|T|/CB = 1$ originate from the unilateral slip mechanisms within the interface $A'A$.

– $\mathbf{e/B = 0}$, the curved portions (cycloids) have been described in paragraph 4.2 (*Fig.* 8) and come from the unilateral mechanisms of Figure 4. They can also be viewed as being representative of mechanisms B and B' when α tends to β.

– $\mathbf{e/B = 0.1}$, the curve for $\delta > 0$ comes from the mechanisms A or B, since for this value of e/B, point I of the best mechanisms is practically coincident with A' ($\beta = \pi/2$ for the mechanism B); for $\delta < 0$, the mechanisms D are the leading ones.

– $\mathbf{e/B = 0.2}$, the curve for $\delta > 0$ comes from the mechanisms A; for $\delta < 0$, the mechanisms D are again the leading ones.

– $\mathbf{e/B = 0.3}$, the curve for $\delta > 0$ comes from the mechanisms A; for $\delta < 0$, the curve is defined by the mechanisms C or D, since point a in the optimal mechanisms is practically coincident with A'.

– $\mathbf{e/B = 0.4}$, the curve for $\delta > 0$ comes from the mechanisms B; the horizontal portion of this curve also delimits the bearing capacity for $\delta < 0$ with an arc arising from the mechanisms C.

From Figure 16, it appears that for e/B =0.1, 0.2 and 0.3, the angular point corresponding to the intersection of the curves arising from the mechanisms A and D, is located on the axis N; moreover, this point is associated with the maximum value of the normal component of the bearing capacity. This result does not as yet have any theoretical basis and this must be considered when taking the accuracy of the numerical minimizations into account.

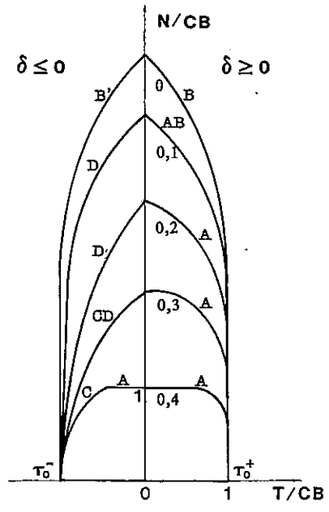

Fig. 16. – Inclined eccentric load: kinematic approaches using mechanisms A, B, C, D, E and their symmetrical solutions for various e/B values.

It is worth noting that the evolution of the leading mechanisms with increasing load eccentricity, and as a function of inclination, is in agreement with the most likely intuitive failure modes. It must also be recalled that curves identical to the curves $IJKL$ of mechanism A (*Fig.* 11) or Aa of mechanism C (*Fig.* 13), are used as failure surfaces in the stability analyses computer programs developed at NGI [Lacasse, 1985; Andersen-Lauritzen, 1988]; experimental evidence regarding similar mechanisms had been obtained by Tran Vo Nhiem (1965) on reduced scale models using Schneebeli rolls.

For a different interface strength criterion (for instance, Coulomb friction), mechanisms with a velocity discontinuity across the interface must be considered. It can be easily verified that the diagrams given in Figure 16 would be truncated by similar curves representing the interface criterion expressed as a function of N/CB and T/CB as in Figure 9 (for a Coulomb friction: $|T|/CB \leq N \tan \phi_i/CB$).

5.3. Ultimate bearing capacity for an inclined eccentric load

The comparison between both approaches is presented in Figure 17, which shows, for each e/B value, the upper and lower bound estimates for the ultimate bearing capacity.

As the eccentricity increases, the gap between the bounds significantly increases. However, as shown in Figure 10, by taking advantage of the convexity properties, the gap has been considerably reduced, compared with what it would be if the reduced width foundation method was used alone. It is likely that the construction of new stress fields applied to the static approach "from inside" would probably tend to reduce the gap even more, especially for positive values of δ. Along these lines, it is worth noting that

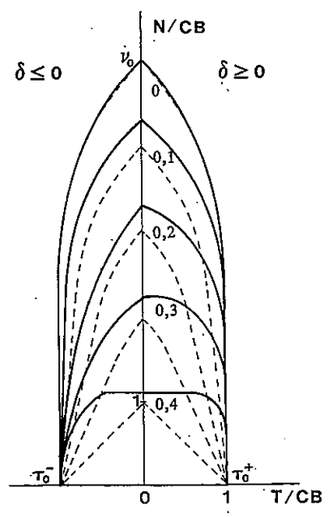

Fig. 17. – Bearing capacity under inclined eccentric load.
Solid lines: upper bound estimates. Dotted lines: lower bound estimates.

the constructed stress fields yield symmetrical diagrams for the lower bounds in T and $-T$, in the (N, T) plane, whereas the upper bounds diagrams are asymmetric (as could intuitively be anticipated for the bearing capacity itself).

Whatever the eccentricity, the bearing capacity is computed exactly for a nil axial load ($N = 0$): points τ_0^+ and τ_0^- in Figure 17.

Once again, attention must be drawn to the importance of the strength condition assumed for the interface, especially with regards to the latter result. All diagrams in Figure 17 should be truncated by the curves expressing the interface strength condition on σ_{yy} and σ_{xy} in terms of N/CB and T/CB: for instance, for a Coulomb interface with a friction angle ϕ_i, $|T|/CB \leq N \operatorname{tg} \phi_i/CB$. This may result in a significant reduction.

6. Conclusions

The present study, conducted within the framework of yield design theory, refers only to the necessary compatibility between the equilibrium of the system under study and the strengths of the constitutive materials. It therefore incorporates the concept of constitutive materials, not only the materials in their usual definition–*i.e.* the foundation soil–, but also any element for which a strength condition governing the system stability is set forth–*i.e.* the soil foundation interface. The theory results in a unique, mathematically simple, formalism, whose practical use calls for the construction of stress fields over the whole system and for the construction of velocity fields or mechanisms.

The interpretation of the results, within this framework, is not ambiguous: they are lower or upper bounds for the ultimate bearing capacity.

This line of thought incorporates both limit analysis and limit equilibrium methods of soil mechanics [Chen, 1975], [Swami Saran and Agarwal, 1991]. The former methods mostly fall within the scope of kinematic approaches. The latter usually appear as partial static analyses along the lines of those developed by [Hill, 1950] or [Sokolovski, 1960, 1965]. It is recalled that [Bishop, 1953] presented a pertinent analysis for the interpretation of the results of such approaches.

On this simple basis, new problems have been treated: load eccentricity and load inclination, parameters which are seldom treated simultaneously [Swami Saran and Agarwal, 1991]. The problem for a material with a tension cut-off in the strength criterion has been solved in [Pecker-Salençon, 1991a], and in the companion paper [Salençon-Pecker, 1995]. Since both cases studied represent extreme conditions for the tensile resistance for the purely cohesive soil, it can be stated that the results bracket the variations of the bearing capacity as a function of the soil tensile strength.

The foundation ultimate bearing capacity has been computed, exactly or with a very high degree of accuracy, for a centered load. For an eccentric load, the bearing capacity has been bracketed between lower and upper bounds as a function of the load eccentricity and load inclination. In view of the safety factors used in the design of foundations under vertical, centered, loads, the inclinations and eccentricities considered in practical applications are usually small.

The results presented herein have been used for the seismic analyses of foundations and are reported in [Pecker and Salençon, 1991b].

Acknowledgments

This study was partially made possible as a result of a grant from the French Ministry of Research and Technology (grant 88F0212) whose support is gratefully acknowledged.

REFERENCES

ANDERSEN K. H., LAURITZSEN R., 1988, *Bearing capacity for foundations with cyclic loads*, Publication No. 175, N.G.I., Oslo.

BISHOP J. F. W., 1953, On the complete solution to problems of deformations of a plastic rigid material, *J. Mech. Phys. Solids*, **2**, 1, 43-53.

CHEN W. F., 1975, *Limit analysis and soil plasticity*, Elsevier Sc. Publ. Cy.

GIROUD J. P., TRAN VO NHIEM, OBIN J. P., 1973, *Tables pour le calcul des fondations*, tome III, Dunod, Paris.

HANSEN B. J., 1961, A general formula for bearing capacity, *Bull. 8, Danish Geotechnical Institute*, Copenhagen.

HANSEN B. J., 1970, A revised and extended formula for bearing capacity, *Bull. 28, Danish Geotechnical Institute*, Copenhagen.

HILL R., 1950, *The mathematical theory of plasticity*, Clarendon Press, Oxford.

KHOSRAVI Z., 1983, Étude théorique et expérimentale de la capacité portante des fondations superficielles, *Thèse Dr. Ing., École Nationale des Ponts et Chaussées*, Paris.

LACASSE S., 1985, Private communication.

MEYERHOF G. G., 1953, The bearing capacity of foundations under eccentric inclined loads, *Proc. 3rd Int. Conf. Soil Mech. Found. Eng.*, Zurich, **1**, 440-445.

MEYERHOF G. G., 1963, Some recent research on the bearing capacity of foundations, *Canadian Geotechnical Journal*, **1**, 1, 16-21.

MIRZABEKIAN, 1979, Generalization of the Prandtl problem of indentation of a die to the case of force eccentricity, *Izv. ANSSSR. Mekhanica Tverdogo Tela*, **14**, 5, 127-138.

PECKER A., SALENÇON J., 1991a, Détermination de la capacité portante des fondations superficielles sous sollicitations dynamiques, *C. R. Recherche M.R.E.S.*, 88-F-0212.

PECKER A., SALENÇON J., 1991b, Seismic bearing capacity of shallow strip foundations on clay soils, *CENAPRED, Proceedings of the International Workshop on Seismology and Earthquake Engineering*, Mexico, April 1991.

PHILIPS A., 1956, *Introduction to Plasticity*, Ronald Press Cy., New York.

PRANDTL L., 1923, Anwendungbeispiele zu einem Henckyschen Satz über das plastiche Gleischgewicht, *Z. Angew. Math. Mech.*, **3**, 401.

SALENÇON J., 1969, La théorie des charges limites dans la résolution des problèmes de plasticité en déformation plane, *Thèse D. Sc.*, Paris.

SALENÇON J., 1973, Prolongement des champs de Prandtl dans le cas du matériau de Coulomb, *Archives of Mechanics*, **25**, 4, 643-648.

SALENÇON J., 1983, *Calcul à la rupture et analyse limite*, Presses de l'E.N.P.C., Paris.

SALENÇON J., 1993, Yield design: a survey of the theory, In *Evaluation of the global bearing capacities of structures*, ed. by G. Sacchi-Landriani, J. Salençon, Springer Verlag, Wien-New York.

SALENÇON J., PECKER A., 1995, Ultimate bearing capacity of shallow foundations under inclined and eccentric loads; Part II: purely cohesive soil without tensile strength, *European Journal of Mechanics A/Solids*, **14**, 2, 377-396.

SAYIR M., ZIEGLER M., 1968, Zum Prandtlschen Stampelproblem, *Ingenieur Archiv.*, **36**, 5, 294-302.

SHIELD R. T., 1954, Plastic potential theory and Prandtl bearing capacity solution, *J. Appl. Mech., trans. ASME*, **21**, 193-194.

SOKOLOVSKI V. V., 1960, *Statics of soil media*, Butterworths, London.

SOKOLOVSKI V. V., 1965, *Statics of granular media*, Pergamon Press, New York.

SWAMI SARAN, ARGAWAL R. K., 1991, Bearing capacity of eccentrically obliquely loaded footing, *J. Geotechnical Eng.*, **117**, 11, 1669-1690.

TRAN VO NHIEM, 1965, Contribution à l'étude de la force portante limite des fondations superficielles dans un milieu à deux dimensions: fondations à charge inclinée et excentrée et fondations sur talus, *Thèse D. Spécialité*, Grenoble.

TRAN VO NHIEM, 1968, Terme de surface de la force portante limite d'une fondation à charge inclinée excentrée par la méthode du coin triangulaire minimal, *C. R. Acad. Sci.*, Paris, **267**, 137-140.

TRAN VO NHIEM, 1971, *Force portante limite des fondations superficielles et résistance maximale à l'arrachement des ancrages*, Thèse Dr. Ing. Faculté des Sciences de Grenoble.

(Manuscript received September 6, 1993;
revised March 23, 1994;
accepted December 23, 1994.)